Variability of Nares Strait ice flux

Ron Kwok

Jet Propulsion Laboratory, California Institute of Technology, Pasadena, California, USA

Received 26 September 2005; revised 14 November 2005; accepted 22 November 2005; published 31 December 2005.

[1] Six years (1996–2002) of Arctic Ocean ice flux into the Nares Strait are estimated using RADARSAT ice motion. This represents a first consistent multi-year record of Nares Strait outflow for examination of seasonal and interannual variability. Across an ~30 km gate at the entrance to Robeson Channel, the average annual (Sept–Aug) ice area flux is 33×10^3 km^2 and ranges from 16×10^3 km^2 in 2000 to 48×10^3 km^2 in 1999. Uncertainties in the 3-day ice displacements and ice flux are small. Assuming 4 m thick ice, the average volume flux amounts to ~130 km^3 (~4 mSv); this is ~7% of the mean annual Fram Strait ice flux. Seasonally, ice flux is most active after July, ceases after the formation of an ice arch in mid- to late-winter, and re-commences after breakup in summer. The multiyear (MY) ice coverage of the area poleward of the gate is high (>80%). South of the gate, the MY ice coverage is highly variable and the strait may be filled with multiyear or seasonal ice. Our estimates are placed in the context of others and uncertainties in the other components of Canadian Archipelago ice flux ~~and~~ are discussed. **Citation:** Kwok, R. (2005), Variability of Nares Strait ice flux, *Geophys. Res. Lett.*, *32*, L24502, doi:10.1029/2005GL024768.

1. Introduction

[2] One pathway of Arctic Ocean sea ice export is through Nares Strait - a relatively narrow passage between the Lincoln Sea and Baffin Bay. This ice volume flux represents a negative term in the annual Arctic Ocean mass balance and the associated meltwater could serve as a source of buoyancy for the upper layers of Baffin Bay. It is considered one component of the net freshwater inflow from the Canadian Arctic Archipelago into Baffin Bay that could potentially weaken deep convection in the Labrador Sea farther downstream [*Goosse et al.*, 1997].

[3] Rough estimates of ice flux have been provided by several investigators [*Dunbar*, 1973; *Sadler*, 1976; *Dey*, 1981; *Agnew*, 1998] and recently summarized by *Tang et al.* [2004]. These earlier results have been based on general estimates of ice motion and thickness derived from coarse satellite imagery (~1 km), reconnaissance flights, ship observations and field programs. The uncertainties in these estimates are not quantified. For narrow passages like the Nares Strait, the spatial resolution of satellite imagery is crucial for accurate determination of the motion field. RADARSAT with its wide-swath coverage, spatial resolution (~100 m) and frequent repeats is ideal platform for providing systematic observations of ice motion at this length scale. Additionally, clouds do not affect the radar imagery. The present note examines the seasonal and interannual variability of the Arctic Ocean sea ice outflow at the Nares Strait using a 6-year record of RADARSAT ice motion. The results are discussed and our estimates of mass outflow are placed in context with estimates from earlier investigations.

0094-8276/05/2005GL024768$05.00

2. Data Description

[4] Ice flux is estimated at a gate positioned at the entrance to Nares Strait (Figure 1) from the Lincoln Sea. The ~30 km gate spans the width of the Robeson channel between Ellesmere Island and Greenland. Ice motion is derived from RADARSAT SAR imagery (resolution: ~150 m) by computing the displacement of common ice features in time-separated images using an image matching procedure described by *Kwok et al.* [1990]. Between 1996 and 2002, the available repeat coverage of Nares Strait is nominally 3 days although a small fraction of motion estimates are over a longer period. The 3-day ice motion is sampled on a 5-km grid that covers a region of ~30 km to the north and south of the gate. All motion vectors are visually inspected for quality and corrected or replaced where needed.

[5] Area flux is computed by first interpolating the gridded ice motion to the gate and then integrating the gate-perpendicular component of the motion profile using the trapezoidal rule. Solid dots (●) show area flux (Figure 2) computed using motion vectors within 5 km of the gate and open circles (o) include vectors more than 5 km away. Due to gradients in ice motion, flux estimates using measurements in proximity of the gate (within 10 km) have lower uncertainty. The motion profile is constrained to go to zero at the coastal endpoints. The expected uncertainty in the displacements is ~300 m. If we assume that the errors of the motion samples to be additive, unbiased, uncorrelated and normally distributed, the uncertainties in the area flux over any a given time interval, σ_F, can be computed viz. [*Kwok and Rothrock*, 1999]: $\sigma_F = \sigma_u L/\sqrt{N_s}$, where L is the width of the flux gate, σ_u is the standard error in the displacement estimates and N_s is the number of independent samples. For $N_s = 6$ (number of 5 km samples along the 30 km gate) and $\sigma_u = 300$ m, the uncertainty in area flux is ~4 km^2 over the sampling interval. This is a small fraction of the average daily flux of ~100 km^2.

[6] Winter ice conditions in Robeson Channel, within the polygon south of the flux gate (in Figure 1), are characterized using ice types. The coverage of the two primary ice types (first-year and multiyear ice) is derived from RADARSAT imagery using a backscatter-based procedure [*Kwok et al.*, 1992] that exploits the large contrast in scattering cross-section between the two ice types. This procedure classifies each SAR image pixel as a member of one of these two types. Broad assessments of the quality of

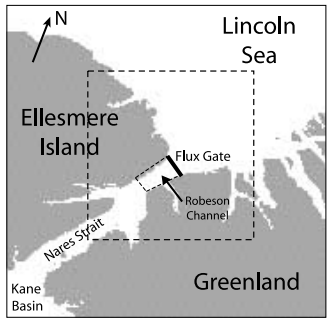

Figure 1. Location of Nares Strait. Flux gate, at the entrance to Robeson Channel, spans the width of ~30 km between Ellesmere Island and Greenland. Smaller polygon defines the area over which the multiyear ice coverage is estimated. Larger box shows the area covered by RADARSAT imagery in Figure 2.

these estimates can be found in work by *Kwok and Cunningham* [2002] and have been shown to be relatively robust during the winter.

3. Results and Discussion

3.1. Ice Drift and Multiyear Ice Coverage

[7] The 6-year record of area flux and MY ice fraction are shown in Figure 2. The first year's record is incomplete and the temporal density of flux estimates is lower than other years. The monthly mean motion profiles and their variability are shown in Figure 3.

[8] The most striking seasonal feature in the time series is that ice flux ceases in mid- to late-winter (lat November to late March), and re-commences after breakup in summer (July and August). This cessation of ice drift through the Strait can be attributed to the formation of an ice arch associated with convergence of thick MY ice onto this funnel-like opening at the entrance into the Strait. Once formed, its structural strength is able to withstanding ice pressures for the duration of the remaining winter and spring. This effectively dams up the Arctic ice cover and stops further Arctic ice export. Figure 2 shows the character of the ice arch after the cessation of ice drift in RADARSAT imagery. Periods of zero-drift vary from 80 days (mid-March till end of May) in 1998 to 220 days (mid-Nov till end of June) in 2000. The atmosphere/ice/ocean conditions conducive to the formation of the ice arch, its persistence, and its disintegration are interesting because it is one of the controlling factors of Arctic ice export, but its examination is beyond the scope of this note.

[9] The cessation of ice drift allows an area of landfast ice to form south of the arch that covers most of Robeson Channel (polygon in Figure 1). As can be seen in the record of MY fraction, this fast ice consists of a mixture of FY and MY ice. This mixture remains relatively unchanged after the cessation of flow. For instance, the MY fraction stayed at a relatively constant fraction of 0.18 in 2000 and at 0.75 in 2002. Occasionally, some of that fast ice in the southern end of Robeson Channel may break off and cause small changes in the ice type mixture. But, these are small compared to the variability in MY fraction before the formation of fast ice in the channel. After summer breakup around July, the channel may have low ice concentration but discrimination of open water/ice in SAR imagery is difficult during this period.

[10] The motion profiles (in Figure 3) show the variability in ice speed at the flux gate. Ice drift direction is predominantly in the direction of Baffin Bay. Occasional northward drifts can be seen in the motion dataset; the variability of the August profile shows a northward excursion. The largest variability in speed is seen between the months of September and November where mean speeds of 20 km/day with variability upwards of 40 km/day can be seen near the center of the gate. Drift speeds are typically lower poleward of the flux gate and highlight the unique atmospheric forcing over the Strait. As a point of reference, the mean daily drift of the thick ice north of the Lincoln Sea is typically less than 5 km/day – an average based on passive microwave ice motion over the past 20 years. South of the gate, the MY ice coverage is highly variable and the

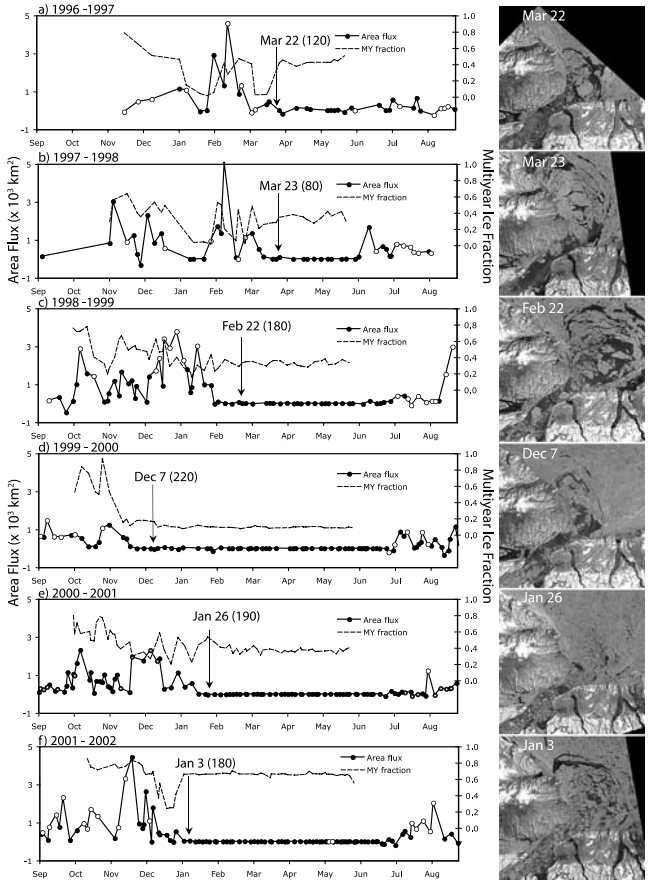

Figure 2. Time series of ice area flux (1996–2002), multiyear ice fraction within the polygon shown in Figure 1, and RADARSAT imagery showing the ice arch following the cessation of ice export during each winter: (a) 96/97, (b) 97/98, (c) 98/99, (d) 99/00, (e) 00/01, and (f) 01/02. The length of the period with no drift (in days) follows the imagery date. Nominally, each flux estimate represents the net area over 3 days although some estimates may be longer. Typically, only motion vectors within 5 km of the gate are used. Open circles indicate estimates where motion vectors more than 5 km from the gate are used resulting in higher uncertainties in these estimates. (RADARSAT imagery ©Canadian Space Agency 2004.)

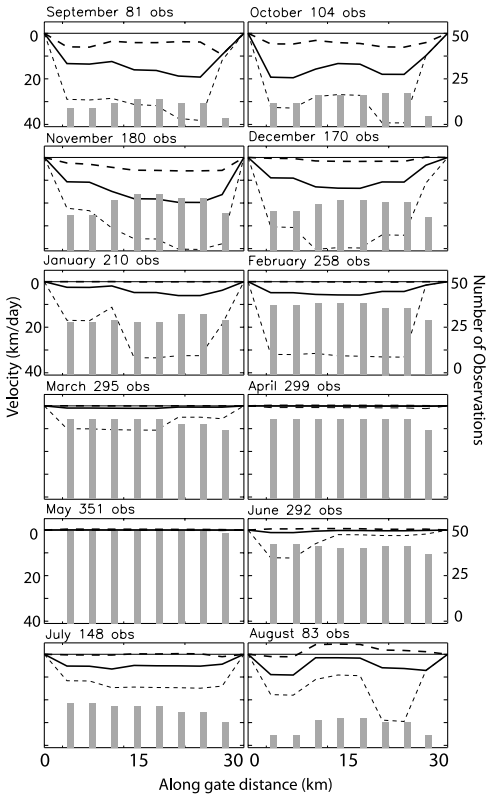

Figure 3. Monthly profiles of ice motion perpendicular to the flux gate. Solid and dashed lines show the mean and variability over the six years. The dashed lines bound the 1-σ (asymmetric) distribution of the motion data about the mean monthly motion. Gray bars show the number of observations used in the computation. The length of the gate is measured from its western endpoint on Ellesmere Island.

compactness of the MY cover is reduced. Individual floes, small enough to fit through the channel, can be seen to break off from the consolidated Arctic pack before flowing through the channel. Flushing of the channel of MY ice can sometimes be associated with periods of large outflows. Drift speeds are dependent on local winds and currents and coastal geometry. The Nares Strait passage is bounded by orographic features reaching 500–2000 m on both sides, which tend to channel surface winds along the strait; strong drainage and katabatic winds from nearby outlet glaciers also contribute to the local surface wind forcing. This helps to explain the large observed drift rates. A recent examination of atmospheric control of sea ice motion in Nares Strait (R. M. Samelson et al., Evidence for atmospheric control of sea ice motion through Nares Strait, submitted to *Geophysical Research Letters*, 2005) suggests that the low-level along strait winds are strongly ageostrophic and may be usefully estimated from pressure differences along the Strait. In addition to wind forcing, *Sadler* [1976] reports that large sea ice floes and icebergs from adjacent outlet glaciers may occasionally block or slow down ice drift in the Robeson Channel.

3.2. Area and Volume Flux

[11] The annual area and volume flux estimates are shown in Figure 4. The average annual (Sept–Aug) ice area flux is 33×10^3 km^2 and ranges from 16×10^3 km^2 in 99/00 to 48×10^3 km^2 in 98/99. The net area ice flux over a season seems to be controlled be three factors discussed above: 1) local surface winds and currents; 2) the length of the period of ice flux cessation in winter and the breakup in late spring; 3) intermittent blockages in the channel that slow or stop ice drift. The length of the 'no-drift' period in part explains the low in 99/00.

[12] Given the relatively high quality of RADARSAT ice drift, the highest uncertainty in the estimation of volume flux is the ice thickness near the flux gate. In their volume estimates, both *Dunbar* [1973] and *Dey* [1981] take ~2.5 m to be a reasonable estimate of the average ice thickness. *Sadler* [1976] uses a thickness of 4.5 m (with an estimated uncertainty of 1 m) for the ridged multiyear ice in Robeson Channel but the average thickness is weighted by the local ice concentration in July and August before estimating the volume flux. *Agnew* [1998] assumes the thickness of MY ice to be 6 m. Recent helicopter borne electromagnetic measurements by *Haas et al.* [2006] in the Lincoln Sea indicate mean thicknesses of 4.7 and 5.2 m in 2004 and 2005. In the absence of any record of ice thickness near Robeson Channel over the same years, we take the mixture of FY and MY ice to have an average thickness of 4(±0.5) m. The 0.5 m was intended to show the magnitude of uncertainty rather than based on actual measurements. With this, we obtain an average annual volume flux of ~130 km^3 (~4 mSv). The variability in flux is high and ranges from a low of 64 km^3 in 99/00 to a high of 193 km^3 in 98/99. This is ~7% of the mean annual Fram Strait ice flux of 1900 km^3 between 1978 and 2003.

[13] Our annual average of 130 km^3 can be compared to the earlier export estimates of 75 km^3, 110(±50) km^3, 65 km^3, 135 km^3 given by *Dunbar* [1973], *Sadler* [1976], *Dey* [1981], and *Agnew* [1998]. Even though these estimates agree remarkably well considering the rough assumptions of ice thickness and ice drift, the high interannual variability seen here is notable. It should be also be noted that the above flux estimates are localized to the Robeson Channel gate and that the estimated values would be different at the exit in the southern end of Smith Sound or the entrance to Baffin Bay. In the summer, consideration of melt during the transit of the Arctic sea ice through the Nares Strait needs to be considered while seasonal ice

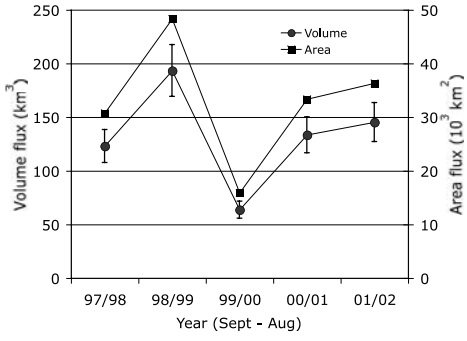

Figure 4. Estimates of annual ice volume flux assuming a mean ice thickness of 4 (±0.5) m. Only five years are shown, as the area flux time series for the first year is incomplete.

production in the Kane Basin and Smith Sound need to be added to the ice volume if flux at this gate is of interest.

4. Conclusions

[14] The present note examines a 6-year record of area and volume outflow of Arctic Ocean sea ice into Nares Strait with RADARSAT data. Routine high-resolution SAR coverage provides the capability to monitor the fairly high drift speeds, the period of no drift, and multiyear ice fraction in narrow channels like the Nares Strait. Using the derived drift, we estimate an average annual (Sept–Aug) ice area flux of 33×10^3 km^2 and an average annual volume flux of $\sim$130 km^3 ($\sim$4 mSv). Interannual variability is high (64 km^3 to 193 km^3). The mean flux can be compared to a recent direct estimate of freshwater flux of 29($\pm$12) mSv through this strait (A. Münchow et al., Observational estimates of volume and freshwater fluxes leaving the Arctic Ocean through Nares Strait, submitted to *Journal of Physical Oceanography*, 2005). It should be noted that the ice component of the Arctic outflow is seasonal because of the cessation of drift in the winter and spring.

[15] On a broader context, the significance of this ice volume export on the mass and heat balance of the Arctic Ocean seems small ($\sim$2 cm of ice thickness – volume flux divided by area of Arctic Ocean) compared to that of the Fram Strait ($\sim$30 cm). Of more interest is perhaps the impact of this export on the hydrography of Baffin Bay and its potential effect on convective overturning downstream in the Labrador Sea. The annual net ice flux from the Canadian Archipelago includes contributions from primarily the Robeson Channel, Jones and Lancaster Sounds. *Sadler* [1976] estimates this flux to be 220 km^3 while *Dey* [1981] gives a much larger estimate of 655 km^3; the Nares Strait flux estimated here could be half or one-sixth of the ice flux from the Canadian Archipelago. This underscores the considerable uncertainty in this quantity. Locally, this can be compared to the estimates of 500 km^3 [*Cuny et al.*, 2005] and 870 km^3 [*Tang et al.*, 2004] of sea ice exported through Davis Strait into the Labrador Sea to the south. For refining these estimates, the focused measurement program of CATS (Canadian Archipelago Throughput Studies) will provide some of the ice drift and thickness needed for satisfying the observational requirements. From remote sensing, we have shown the efficacy of ice drift derived from high resolution SAR imagery. The ice thickness requirement is more difficult to address; perhaps the freeboard estimates from spaceborne altimeters like ICESat [*Kwok et al.*, 2004] or ERS/Envisat [*Laxon et al.*, 2003] would augment airborne/field campaigns and point measurements from upward looking sonars.

[16] Given the uncertainties in the ice budget in Baffin Bay, the effect and role of sea ice imported through the Canadian Archipelago on the convective overturning downstream in the Labrador Sea remain a question. Here, we addressed partly the Robeson Channel term of that equation.

[17] **Acknowledgments.** I wish to thank S. S. Pang for her assistance during the preparation of this manuscript. The RADARSAT imagery is provided by the Alaska Satellite Facility, Fairbanks, AK. This work was performed at the Jet Propulsion Laboratory, California Institute of Technology and is sponsored by the National Science Foundation and the National Aeronautics and Space Administration.

References

Agnew, T. A. (1998), Drainage of multiyear sea ice from the Lincoln Sea, *Can. Meteorol. Oceanic Soc. Bull.*, *26*(4), 101–103.

Cuny, J., P. Rhines, and R. Kwok (2005), Davis Strait fluxes, *Deep Sea Res. Part I*, *52*(3), 519–542.

Dey, B. (1981), Monitoring winter sea ice dynamics in the Canadian Arctic with NOAA-TIR images, *J. Geophys. Res.*, *86*, 3223–3235.

Dunbar, M. (1973), Ice regime and ice transport in Nares Strait, *Arctic*, *26*, 282–291.

Goosse, H., T. Fichefet, and J.-M. Campin (1997), The effects of the water flow through the Canadian archipelago in a global ice-ocean model, *Geophys. Res. Lett.*, *24*, 1507–1510.

Haas, C., S. Hendricks, and M. Doble (2006), Comparison of the sea ice thickness distribution in the Lincoln Sea and adjacent Arctic Ocean in 2004 and 2005, *Ann. Glaciol.*, in press.

Kwok, R., and G. F. Cunningham (2002), Seasonal ice area and volume production of the Arctic Ocean: November 1996 through April 1997, *J. Geophys. Res.*, *107*(C10), 8038, doi:10.1029/2000JC000469.

Kwok, R., and D. A. Rothrock (1999), Variability of Fram Strait flux and North Atlantic Oscillation, *J. Geophys. Res.*, *104*, 5177–5189.

Kwok, R., J. C. Curlander, R. McConnell, and S. Pang (1990), An ice motion tracking system at the Alaska SAR facility, *IEEE J. Oceanic Eng.*, *15*(1), 44–54.

Kwok, R., E. Rignot, B. Holt, and R. G. Onstott (1992), Identification of sea ice type in spaceborne SAR data, *J. Geophys. Res.*, *97*, 2391–2402.

Kwok, R., H. J. Zwally, and D. Yi (2004), ICESat observations of Arctic sea ice: A first look, *Geophys. Res. Lett.*, *31*, L16401, doi:10.1029/2004GL020309.

Laxon, S., N. Peacock, and D. Smith (2003), High interannual variability of sea ice in the Arctic region, *Nature*, *425*, 947–950.

Sadler, H. E. (1976), Water, heat, and salt transports through Nares Strait, Ellesmere Island, *J. Fish. Res. Board Can.*, *33*, 2286–2295.

Tang, C. L., C. K. Ross, T. Yao, B. Petrie, B. M. DeTracey, and E. Dunlap (2004), The circulation, water masses and sea-ice of Baffin Bay, *Prog. Oceanogr.*, *63*, 183–228.

R. Kwok, Jet Propulsion Laboratory, California Institute of Technology, 4800 Oak Grove Drive, Pasadena, CA 91109, USA. (ron.kwok@jpl.nasa.gov)